VENTRICULAR AND ARTERIAL WALL STRESSES BASED ON LARGE DEFORMATION ANALYSES

I. MIRSKY

From the Department of Medicine, Division of Mathematical Biology, Harvard Medical School and Peter Bent Brigham Hospital, Boston, Massachusetts 02115

ABSTRACT Assuming a spherical geometry for the left ventricle and a cylindrical geometry for arteries, wall stresses and elastic stiffnesses are evaluated on the basis of a large elastic deformation theory. On the basis of canine pressure-volume data, the numerical results indicate marked gradients of stress in the endocardial layers even for thin-walled vessels, a result not predicted by the classical theory of elasticity. These high gradients of stress are due to the fact that the elastic stiffness of the wall material increases with the stress which reaches maximum levels in the endocardial layers. The high stresses may be responsible for ischemia of the left ventricle and be a triggering mechanism for atherosclerosis.

INTRODUCTION

Most studies relating to the quantitation of left ventricular wall stresses have been based on the classical theory of elasticity (Wood, 1892; Burch et al., 1952; Burton, 1957; Sandler and Dodge, 1963; Ghista and Sandler, 1969; Wong and Rautaharju, 1968; Mirsky, 1969, 1970; Streeter et al., 1969; Gould et, al. 1972). This theory assumes that elastic deformations are small, i.e., less than 10% of their initial unloaded dimensions. However, it is well known for biological materials that deformations of the order of 50–100% can take place. It is therefore apparent that the classical theory is not adequate to describe the mechanical behavior of biological tissues and the theory must be replaced by a more appropriate one.

The need to obtain a better understanding of the mechanical properties of rubberlike materials has resulted in the rapid development of a finite elastic deformation theory which is capable of describing such large deformations. This theory has already been applied in recent years to biological problems by Fung (1967), Mirsky (1968), Gou (1970), Simon et al. (1971, 1972), and Vaishnav et al. (1972). In particular, Simon et al. (1972) have shown that the stress distribution in thin-walled tubes is far from being uniform, a result that might be expected with the classical elasticity theory in the form of the Laplace Law.

The prime purpose of the present study is to provide a method for quantitating left ventricular wall stresses since recent studies (Monroe et al., 1972; Barnard et al.,

1972) have indicated the presence of ischemia in the canine heart and an unfavorable alteration in the subendocardial oxygen supply demand relationship in the normal human heart. Although the problem of arterial wall stress has previously been considered, a simpler method of analysis is presented here and additional mechanical properties of the arteries are discussed. In particular, it is important to develop methods for evaluating elastic stiffness in both arteries and veins in view of the fact that fibrosis of the intima has been reported after saphenous vein bypass surgery.

THEORETICAL CONSIDERATIONS

For the present analysis we are primarily interested in the qualitative aspects of wall stress distribution. Thus idealized geometries are assumed for both the left ventricle and the arteries. A spherical geometry is assumed for the left ventricle and the arteries and veins are approximated by cylinders constrained at a constant length after pressure inflation.

In each case, the material is assumed to be isotropic, homogeneous, and incompressible. It is recognized that these assumptions are rather crude; however, they are dictated by the fact that experimental data with regard to nonhomogeneity and anisotropy of biological tissues are sparse, although Patel and his associates have quantitated the anisotropic elastic properties in arteries (1969, 1970).

Left Ventricle

Large deformation theory of elasticity is presented in great detail by Green and Zerna (1954) and Green and Adkins (1960) who have studied the particular problems of symmetrical expansion of thick spherical shells and cylindrical tubes initially extended followed by inflation. For completeness of this presentation, the mathematical details will be outlined here for both the ventricle and artery.

Consider a spherical coordinate system (R, θ, φ) in the strained body having its origin at the center of the shell, and let (r, θ, φ) be the coordinate system in the unstrained body. Denoting the internal and external radii of the shell in the unstrained and strained states by r_1, r_2 and R_1, R_2, respectively, the following relations hold as a consequence of the assumption of incompressibility:

$$r^3 - R^3 = r_1^3 - R_1^3 = r_2^3 - R_2^3, \tag{1}$$

$$Q(R) = r/R = \left(1 + \frac{r_1^3 - R_1^3}{R^3}\right)^{1/3}, \tag{2}$$

We now introduce the concept of a strain energy density function denoted by W, which is the amount of mechanical energy required to deform a given volume of material. If this function W is known, the elastic mechanical properties of the material may be determined since they are obtainable from the constitutive relations (stress-strain relations) which are based on the strain energy function.

In general, W is a function of the strain components γ_{ij}, hence $W = W(\gamma_{ij})$ where in particular, γ_{11}, γ_{22}, γ_{33} represent the radial, circumferential, and meridional

components of strain, respectively. For the special case of spherical symmetry of an incompressible material, the strain energy density function may be written as a function of strain invariants which are combinations of the strain components γ_{ij} (Green and Zerna, 1954). For the present analysis, the particular strain invariant I is given in the form

$$I = Q^4 + 2/Q^2, \tag{3}$$

and W is expressed as $W = W(I)$.

In terms of W and Q, the nonzero components of stress are

$$\begin{aligned} \tau^{11} &= 2Q^4 \partial W/\partial I + P_H, \\ R^2\tau^{22} &= (2/Q^2)\partial W/\partial I + P_H, \end{aligned} \tag{4}$$

where τ^{11}, $R^2\tau^{22}$ are the radial and circumferential components of stress, respectively, and P_H is a "hydrostatic pressure" to be determined from the equilibrium and boundary conditions.

The equation of equilibrium for the evaluation of the function P_H is given in the form

$$(\mathrm{d}P_H/\mathrm{d}Q) + Q^4(\mathrm{d}\Phi/\mathrm{d}Q) + 2(Q^3 - 1)\Phi = 0, \tag{5}$$

where $\Phi = 2\,\partial W/\partial I$. On integration we obtain

$$P_H = -Q^4\Phi + 2\int^Q (Q^3 + 1)\,\Phi\,\mathrm{d}Q + C, \tag{6}$$

where C is a constant of integration to be determined from the boundary conditions. For the present analysis, it is assumed that P is the left ventricular pressure and on the epicardial surface, the pressure is zero.

Therefore the boundary conditions are:

$$\tau^{11} = -P \text{ on } R = R_1; \qquad \tau^{11} = 0 \text{ on } R = R_2. \tag{7}$$

These conditions yield the following relations:

$$\begin{aligned} -P &= 2\int^{Q_1} (Q^3 + 1)\,\Phi\,\mathrm{d}Q + C\ (Q_1 = r_1/R_1), \\ P_H &= -Q^4\Phi + K(R) - P, \\ K(R) &= 2\int_{Q_1}^{Q} (Q^3 + 1)\,\Phi\,\mathrm{d}Q, \\ \tau^{11} &= K(R) - P, \\ R^2\tau^{22} &= (1/Q^2 - Q^4)\,\Phi + K(R) - P, \\ K(R_2) &= P. \end{aligned} \tag{8}$$

This latter condition serves to determine R_1 if the pressure P and the strain energy density W are known since R_2 may be expressed in terms of R_1 via the incompressibility condition 1.

It should be noted that expressions 4 for the stress components are analogous to the stress-strain relations in the classical theory of elasticity for an isotropic incompressible material, namely,

$$\sigma_{rr} = \Pi + 2Ge_{rr},$$

$$\sigma_{\theta\theta} = \Pi + 2Ge_{\theta\theta}, \tag{9}$$

where e_{rr}, $e_{\theta\theta}$, σ_{rr}, and $\sigma_{\theta\theta}$ are strain and stress components, Π is the hydrostatic pressure, and G is the shear modulus of elasticity.

The equilibrium condition $K(R_2) = P$ may be better understood by putting it in an alternative form. Now

$$\begin{aligned} K(R) &= 2\int_{Q_1}^{Q} (Q^3 + 1) \cdot 2\partial W/\partial I \, dQ = 4\int_{Q_1}^{Q} (Q^3 + 1)(dW/dQ)(dQ/dI)\, dQ \\ &= \int_{Q_1}^{Q} [Q^3/(Q^3 - 1)]\,(dW/dQ) \text{ since } dI/dQ = 4Q^3 - 4/Q^3 \\ &= \int_{R_1}^{R} \left(\frac{R^3 + r_1^3 - R_1^3}{r_1^3 - R_1^3}\right) \frac{dW}{dR}\, dR. \end{aligned} \tag{10}$$

Hence

$$K(R_2) = [r_2^3 W(R_2) - r_1^3 W(R_1) - (3/4\pi)U]/(r_1^3 - R_1^3) = P, \tag{11}$$

where use has been made of the incompressibility conditions 1 and

$$U = \int_{R_1}^{R_2} 4\pi R^2 W dR \tag{12}$$

is the total elastic energy stored by the spherical ventricle. Alternatively, we may write

$$U = (4\pi/3)(R_1^3 - r_1^3)P + (4\pi/3)r_2^3 W(R_2) - (4\pi/3)r_1^3 W(R_1). \tag{13}$$

Cylindrical Arteries

For the case of the cylindrical arteries, we assume that a uniform simple extension takes place parallel to the axis of the tube. This is followed by a uniform inflation in which the length remains constant and the radii r_1, r_2 in the unstrained state change to R_1, R_2.

If we consider a cylindrical polar coordinate system (R, θ, z) in the deformed state, then the point (R, θ, z) was initially at the point $(r, \theta, z/\lambda)$, where r is a function of R and λ is the ratio of the deformed to the undeformed length. The functional relationship between r and R is obtained from the incompressibility condition with the result that

$$2\pi R \, dR \, dz = 2\pi r \, dr \, dz/\lambda,$$

or

$$r(dr/dR) = \lambda R. \tag{14}$$

Integration of this equation yields

$$r^2 = \lambda(R^2 + K) = R^2 Q^2(R), \tag{15}$$

where K is a constant of integration and $Q = r/R$. Since $r = r_1$ when $R = R_1$ and $r = r_2$ when $R = R_2$,

$$R_1^2 + K = r_1^2/\lambda; \qquad R_2^2 + K = r_2^2/\lambda. \tag{16}$$

Again as in the case of the ventricle, we introduce the strain energy density function W and express the stress components in the form

$$\begin{aligned} \tau^{11} &= P_H + 2(Q^2/\lambda^2)(\partial W/\partial I) \qquad \text{(radial)}, \\ R^2\tau^{22} &= P_H + 2(\partial W/\partial I)/Q^2 \qquad \text{(circumferential)}, \end{aligned} \tag{17}$$

where the strain invariant I is given by

$$I = \lambda^2 + Q^2/\lambda^2 + 1/Q^2. \tag{18}$$

The hydrostatic pressure P_H satisfies the equilibrium equation

$$(d/dR)[P_H + 2(Q^2/\lambda^2)(\partial W/\partial I)] + (2/R)[(Q^2/\lambda^2) - (1/Q^2)](\partial W/\partial I), \tag{19}$$

which on integration yields the expression

$$P_H = -2(Q^2/\lambda^2)(\partial W/\partial I) - L(R) + H, \tag{20}$$

where H is a constant of integration and $L(R)$ is given by

$$L(R) = \int_R^{R_2} \left(\frac{Q^2}{\lambda^2} - \frac{1}{Q^2}\right)(2\,\partial W/\partial I)\,\frac{dR}{R}. \tag{21}$$

The boundary conditions $\tau^{11} = -P$ on $R = R_1$ and $\tau^{11} = 0$ on $R = R_2$, where P

is the arterial pressure, yield the following relations:

$$H = 0$$

$$L(R_1) = P$$

$$\tau^{11} = -L(R) = \int_R^{R_2} (Q^2/\lambda^2 - 1/Q^2)(2\partial W/\partial I)\, \mathrm{d}R/R \tag{22}$$

$$R^2\tau^{22} = \tau^{11} + 2(\partial W/\partial I)[(1/Q^2) - (Q^2/\lambda^2)].$$

As before, the equilibrium condition $L(R_1) = P$ may be written in terms of the total energy stored elastically in the cylindrical shell as follows:

$$\begin{aligned} L(R_1) &= \int_{R_1}^{R_2} 2(\partial W/\partial I)[(1/Q^2) - (Q^2/\lambda^2)]\, \mathrm{d}R/R, \\ &= 2\int_{R_1}^{R_2} [(1/Q^2) - (Q^2/\lambda^2)](\mathrm{d}R/\mathrm{d}Q)(\mathrm{d}Q/\mathrm{d}I)(\mathrm{d}W/R), \\ &= \int_{R_1}^{R_2} (R^2/K + 1)\, \mathrm{d}W, \\ &= W(R_2) - W(R_1) + [R^2/K - \int 2(WR/K)\mathrm{d}R]_{R_1}^{R_2}, \\ &= (r_2^2/\lambda K)\, W(R_2) - (r_1^2/\lambda K)\, W(R_1) - (2/K)\int_{R_1}^{R_2} RW\mathrm{d}R = P, \end{aligned} \tag{23}$$

or

$$U = P(\pi R_1^2\lambda l_0 - \pi r_1^2 l_0) + (\pi r_2^2 l_0)W(R_2) - (\pi r_1^2 l_0)W(R_1), \tag{24}$$

where l_0 is the undeformed length of the artery and the total energy U is given by

$$U = \int_{R_1}^{R_2} (2\pi\lambda l_0 R)\, W\mathrm{d}R. \tag{25}$$

Evaluation of the Strain-Energy Density Function $\partial W/\partial I$

Case 1: Left Ventricle. For the determination of the function $\partial W/\partial I$, a modified method similar to that employed by Simon et al. (1972) will be adopted here. As a first approximation, $\partial W/\partial I$ will be evaluated from the set of Eqs. 4 employing midwall values for the stress components τ^{11}, $R^2\tau^{22}$ as obtained from the classical theory of elasticity for a thick spherical shell (Timoshenko and Goodier, 1951). These stresses, which are close to average values, may be written in the form

$$\begin{aligned} R_m^2\tau_m^{22} &= P(V/V_w)[1 + 0.5(R_2/R_m)^3], \\ \tau_m^{11} &= P(V/V_w)[1 - (R_2/R_m)^3], \end{aligned} \tag{26}$$

where V is the left ventricular volume, V_w is the left ventricular wall volume, and the subscript m denotes the midwall value. Thus $(\partial W/\partial I)_m$ is given by

$$(\partial W/\partial I)_m = Q_m^2(R_m^2\tau_m^{22} - \tau^{11})/2(1 - Q_m^6),$$

$$= 0.75\, P(V/V_w)(R_2/R_m)^3 Q_m^2/(1 - Q_m^6), \qquad (27)$$

which can be evaluated for each pressure level P if the pressure-volume and pressure-radii data are known. However, in order to determine the stress distribution through the wall of the left ventricle, we require $\partial W/\partial I$ as a function of I (which indirectly is a function of R).

In their studies, Simon et al. (1972) assumed $\partial W/\partial I$ in the exponential form $\partial W/\partial I = Ae^{kI}$ where $\partial W/\partial I$ and I in this instance are midwall values. Furthermore, $\partial W/\partial I$ was evaluated at a given pressure P on the basis of the Laplace Law for a thin cylinder. From a semilog plot of $\partial W/\partial I$ vs. I, they obtained approximate values for the constants A, k. These calculations were repeated for various values of A and k until the pressure-radius response predicted by the equilibrium equation $K(R_2) = P$ agreed with the experimental data. This approach was employed initially in the present study but was abandoned because of the tedious computations.

An alternative approach which is quite accurate and relatively simpler from the computational point of view is outlined here: (*a*) for each pressure level P, $\partial W/\partial I$ is evaluated at the midwall employing relation 27, and (*b*) this value for $(\partial W/\partial I)_m$ is then plotted against I_M which is the average of the values for I at the endocardial and epicardial surfaces, i.e., $I_M = (I_1 + I_2)/2$. The data are fitted to an exponential curve in the form $\partial W/\partial I = A + Be^{CI}$ where A, B, C are constants determined from a nonlinear regression analysis. The constants are then adjusted until the equilibrium condition $P = K(R_2)$ agrees to within 5% of the experimental pressure-radius data.

The justification for adopting midwall values for $\partial W/\partial I$ stems from the fact that the equilibrium condition

$$K(R_2) = \int_{Q_1}^{Q_2} 4(Q^3 + 1)(\partial W/\partial I)\mathrm{d}Q$$

$$= (\partial W/\partial I)_m[(Q_2^4 - Q_1^4) + 4(Q_2 - Q_1)] \qquad (28)$$

yielded values for the pressure P to within 10% when $\partial W/\partial I$ was assumed constant over the range of integration. The rationale for employing an average value I_M rather than I_m stems from the observation that I declines sharply from the endocardial to the epicardial surfaces with the result that I_m takes on values close to I_2.

Case 2: Arteries. A similar procedure is employed for the arterial analysis. For a thick-walled cylinder, the classical theory (Timoshenko and Goodier 1951) yields the following expressions for the midwall radial and circumferential

stresses

$$\tau_m^{11} = P(V/V_w)[1 - (R_2/R_m)^2],$$

$$R_m^2\tau_m^{22} = P(V/V_w)[1 + (R_2/R_m)^2]. \tag{29}$$

Thus $(\partial W/\partial I)_m$ as determined from Eqs. 17 is

$$(\partial W/\partial I)_m = P(V/V_w)(R_2/R_m)^2/\left(\frac{1}{Q_m^2} - \frac{Q_m^2}{\lambda^2}\right). \tag{30}$$

This quantity is plotted against $I_M = (I_1 + I_2)/2$ and curve fitted to an exponential function of the form

$$\partial W/\partial I = A + Be^{CI}. \tag{31}$$

NUMERICAL RESULTS AND DISCUSSION

Left Ventricle

Pressure-volume data obtained from dog studies by Spotnitz et al. (1966) have been employed in the evaluation of left ventricular wall stresses. These data are presented in Table I which includes also the strain energy density $(\partial W/\partial I)_m$ at each pressure level. The first approximation to $\partial W/\partial I$ was determined to be $\partial W/\partial I = -6.9 + 0.4\, e^{0.916I}$ and after several calculations this was modified to

$$\partial W/\partial I = -6.1 + 0.4\, w^{0.98I}. \tag{32}$$

With this expression for $\partial W/\partial I$, the integral expression for $K(R_2)$ was computed at 5 mm Hg pressure increments over the range 5–30 mm Hg. Fig. 1 shows the experimental (P vs. R_1) and calculated [$K(R_2)$ vs. R_1] pressure-radius curves and it is observed that agreement was obtained to within 4% over this pressure range. In

TABLE I

PRESSURE-VOLUME DATA AND STRAIN-ENERGY DENSITY FOR THE LEFT VENTRICLE*

P	V	R_1	R_m	R_2	$(\partial W/\partial I)_m$	I_M
mm Hg	*ml*		*cm*		*mm Hg*	
5	31.5	1.96	2.56	3.15	3.73	3.56
10	40.0	2.12	2.67	3.22	6.82	3.86
15	46.7	2.23	2.74	3.27	9.9	4.1
20	52.0	2.31	2.80	3.31	13.0	4.28
25	56.5	2.38	2.85	3.34	16.1	4.44
30	60.0	2.43	2.90	3.37	19.3	4.56

Wall volume V_w = 100 ml.
At zero pressure, V = 12 ml, R_1 = 1.42 cm, R_2 = 2.99 cm.
* Data obtained from the dog studies by Spotnitz et al. (1966).

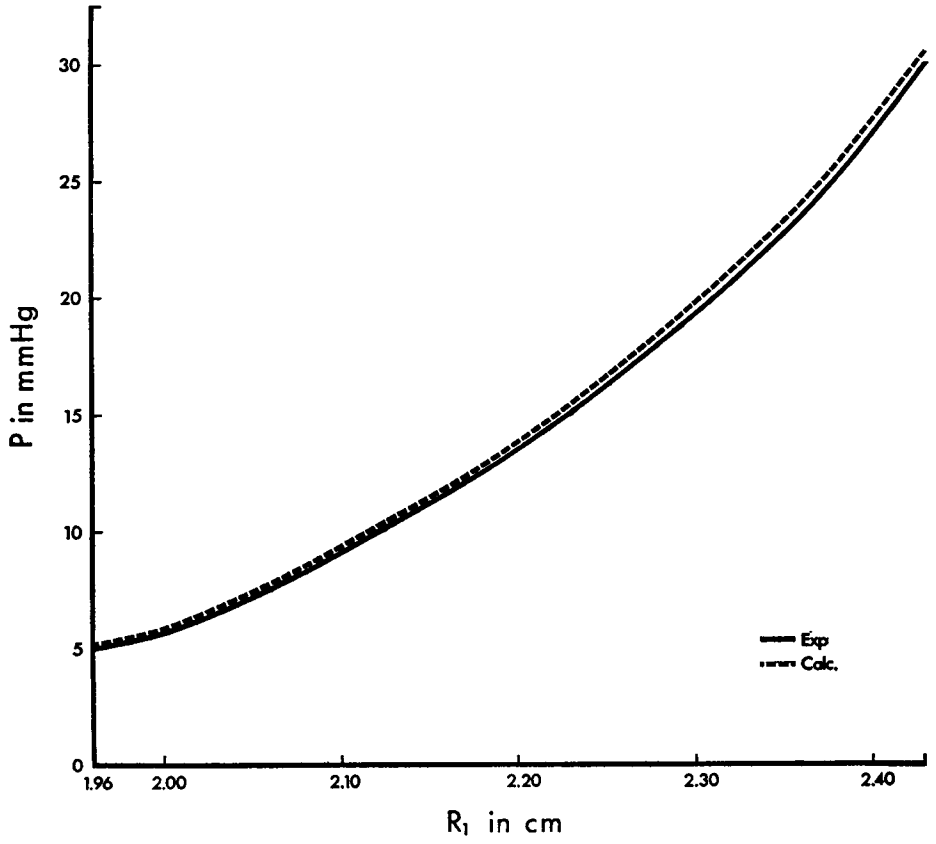

FIGURE 1 Pressure-radius curves for the canine left ventricle. The solid curve is obtained from the studies by Spotnitz et al. (1966). The dotted curve is evaluated from the integral expression 8 for $K(R_2)$. There is agreement between the two curves to within 4%.

Fig. 2 the left ventricular circumferential stress based on both the classical theory and large deformation theory is plotted as a percentage of the wall thickness for a ventricular pressure $P = 20$ mm Hg. The circumferential stresses have been normalized to $(PR_1/2h)$ which is the mean stress as given by the Laplace Law for a sphere (Mirsky, 1969). The marked differences in the stress distributions are quite apparent and there is a 10-fold increase in the stress at the endocardial surface over that predicted by the classical theory.

An approximate expression for the strain energy function $W(I)$ may be obtained on integration of expression 32 with the result that

$$W(I) = C_1 - 6.1\, I + 0.43\, e^{0.98I}, \tag{33}$$

where $C_1 = 11.3$, obtained from the condition $W = 0$ when $I = 3$ (undeformed state). This expression is displayed graphically in Fig. 3 as a function of the wall

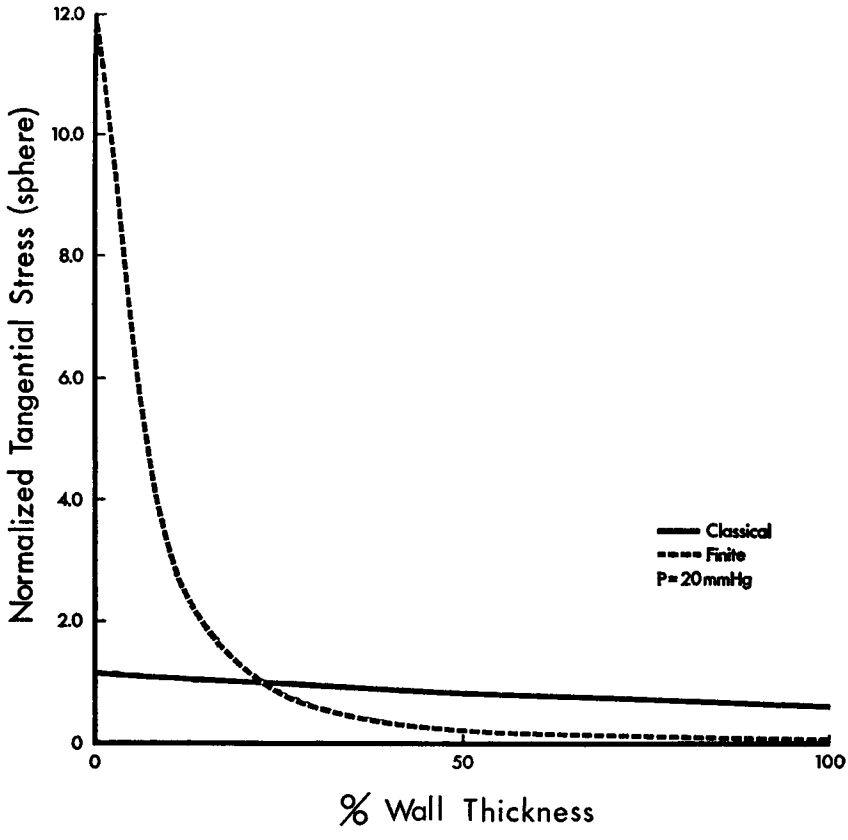

FIGURE 2 Tangential wall stress distributions obtained from classical thick-walled theory and large deformation theory on the basis of a spherical geometry for the left ventricle. The stress is normalized to the Laplace stress for a sphere ($\sigma = PR_i/2h$). Note the marked gradient of stress in the endocardial layers for the finite theory shown by the dotted curve.

thickness for the pressure levels $P = 10, 20, 30$ mm Hg. It can be noted that in the endocardial layers, there are significantly elevated levels in the strain energy which increase more rapidly with an increase in the pressure level. The nonuniformity through the wall thickness of both the wall stress and strain energy is not surprising in view of the fact that for biological materials, elastic wall stiffness increases with the stress as will be shown in the next section and observed in Fig. 4.

Elastic Stiffness of the Left Ventricle. Since there is a wide discrepancy in the stresses as obtained from both the classical theory and finite deformation theory, inaccuracies must also occur in the evaluation of elastic stiffness. In previous studies by Mirsky and Parmley (1972), the elastic stiffness of the left ventricle was obtained from the expression $d\sigma/d\epsilon$ where σ is the midwall circumferential stress based on the classical theory and ϵ is the midwall circumferential strain defined by $d\epsilon = dR_m/R_m$. Alternative expressions are often employed in arterial mechanics and

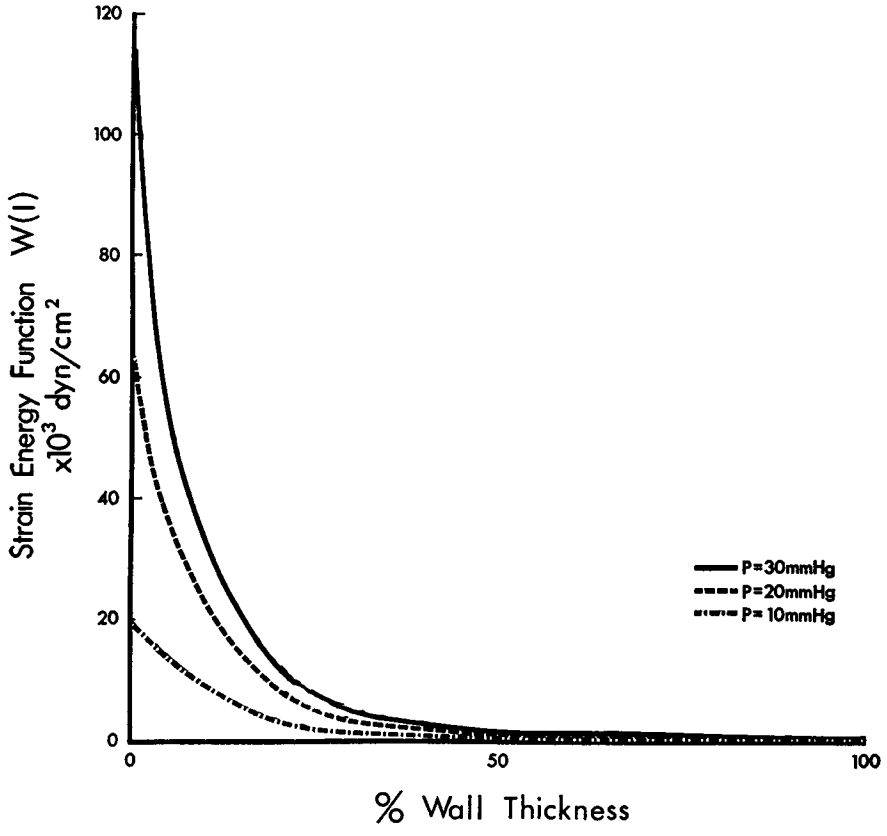

FIGURE 3 Strain energy function $W(I)$ plotted as a percentage of wall thickness. The curves are qualitatively similar to the stress distributions. It should be noted that the gradient in the endocardial layers increases rapidly with an increase in the ventricular pressure P.

in particular, the incremental elastic modulus is defined as

$$E_{\text{INC}} = \frac{3}{2}\frac{(\Delta\sigma_{\theta\theta} - \Delta\sigma_{rr})}{(\Delta e_{\theta\theta} - \Delta e_{rr})}, \tag{34}$$

where $\Delta\sigma_{rr}$, $\Delta\sigma_{\theta\theta}$ are the incremental radial and circumferential stresses, respectively, and Δe_{rr}, $\Delta e_{\theta\theta}$ are the corresponding incremental strains. A derivation of this formula is given in the Appendix.

Unfortunately, there appears to be some confusion as to the choice of formulae for evaluating stiffness. Therefore, several formulae will be outlined here, since the choice is of importance when considering the problem of wave propagation through arteries to be discussed later.

As shown in the Appendix, expression 34 reduces to

$$E_{\text{INC}} = (\Delta\sigma_{\theta\theta} - \Delta\sigma_{rr})/2\Delta e_{\theta\theta}. \tag{35}$$

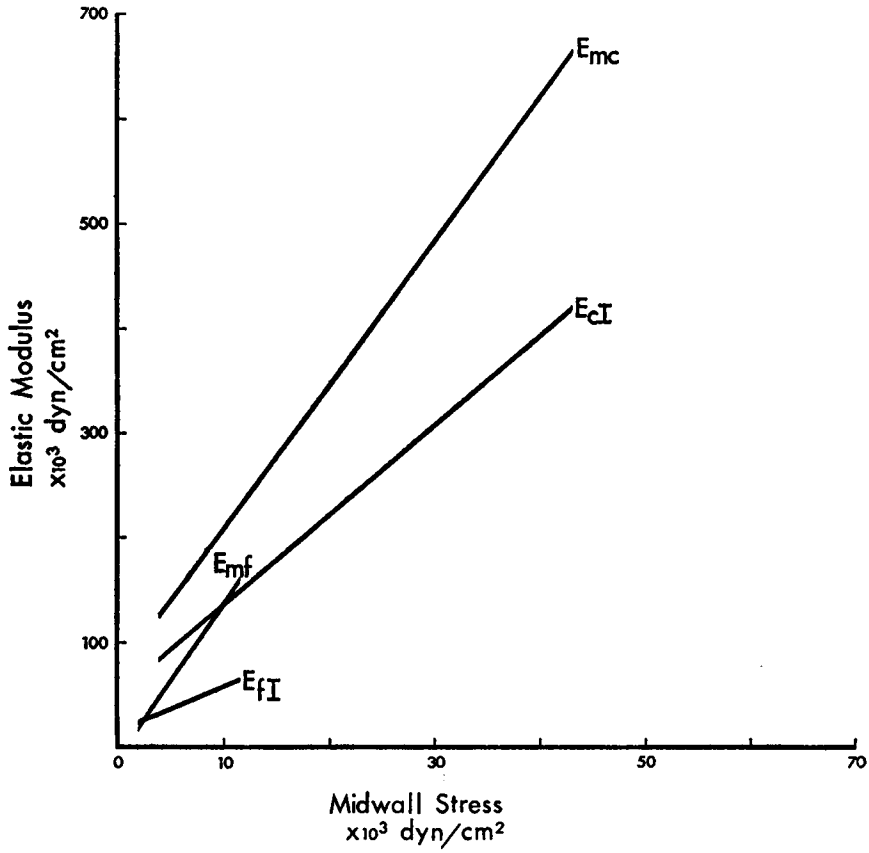

FIGURE 4 The elastic stiffness-stress relations for the left ventricle as obtained from the classical and large deformation theories. E_{mc} and E_{mf} are the elastic stiffness at the midwall based on the classical and finite theories, respectively, employing the formula $R_m\Delta\sigma_{\theta m}/\Delta R_m$. The quantities E_{cI} and E_{fI} are the incremental moduli obtained on the basis of expression 37. In each case, the elastic stiffness based on the finite theory are much lower than those obtained from the classical theory.

With this expression, it is now possible to evaluate the incremental moduli at various locations through the wall thickness as follows: at the endocardial surface, $\Delta\sigma_{rr} = -P, \Delta e_{\theta\theta} = \Delta R_1/R_1$, thus

$$E_1 = (R_1/2)(\Delta\sigma_{\theta 1}/\Delta R_1 + \Delta P/\Delta R_1), \tag{36}$$

where $\sigma_{\theta 1}$ is the endocardial circumferential stress. At the midwall,

$$E_m = (R_m/2)(\Delta\sigma_{\theta\theta} - \Delta\sigma_{rr)m}/\Delta R_m, \tag{37}$$

and finally at the epicardial surface where $\Delta\sigma_{rr} = 0$,

$$E_2 = (R_2/2)\Delta\sigma_{\theta 2}/\Delta R_2. \tag{38}$$

In Fig. 4 the elastic stiffness E_m is plotted against midwall stress $\sigma_{\theta m}$ employing the formula $R_m \Delta\sigma_{\theta m}/\Delta R_m$ and expression 37. These expressions are evaluated on the basis of the classical and large deformation theories. Several points are worthy of note: (*a*) the elastic stiffness bears a linear relationship with the stress, a consequence of the exponential stress-strain relation which is characteristic for biological materials, (*b*) the elastic stiffness constants (represented by the slopes of these lines) based on the formula $d\sigma/d\epsilon$ are similar for both theories, and (*c*) elastic stiffness evaluated from the finite theory is much lower than that based on the classical theory.

On the other hand, if we examine the elastic stiffness values at the endocardial surface, we find that the values predicted by the classical theory are much lower than those given by the large deformation theory. It should be noted that elastic stiffnesses based on the latter theory were not evaluated at the epicardial surface since the stresses here were very small so that small errors in these stresses induced by the various approximations employed could result in large errors in the elastic stiffness. Simon et al. (1972), however, did note large variations at the epicardial surface between the two theories in their studies with arteries. Thus it is important to state the location in the wall when elastic stiffnesses are evaluated. This is particularly of concern in a study of wave propagation velocities in arteries to be discussed in a later section.

Cylindrical Arteries

Elastic Stiffness. As observed for the left ventricle, the elastic stiffness apparently varies through the wall thickness. For an artery maintained at a constant length after the initial stretch, the incremental modulus E_{INC} is (see Appendix)

$$E_{\text{INC}} = (\tfrac{3}{4})(\Delta\sigma_{\theta\theta}/\Delta e_{\theta\theta} - \Delta\sigma_{rr}/\Delta e_{\theta\theta}). \tag{39}$$

Expressions for the incremental moduli at various locations through the wall are given by

$$\begin{aligned} E_1 &= (\tfrac{3}{4})R_1[(\Delta\sigma_{\theta 1}/\Delta R_1) + (\Delta P/\Delta R_1)] && \text{(endocardial)}, \\ E_m &= (\tfrac{3}{4})R_m\Delta(\sigma_{\theta\theta} - \sigma_{rr})_m/\Delta R_m && \text{(midwall)}, \\ E_2 &= (\tfrac{3}{4})R_2\Delta\sigma_{\theta 2}/\Delta R_2 && \text{(epicardial)}, \end{aligned} \tag{40}$$

where the various quantities have been previously defined.

The qualitative differences between the two theories for both the incremental modulus and the elastic stiffness given by the expression $E = \Delta\sigma_{\theta\theta}/\Delta e_{\theta\theta} = R\Delta\sigma_{\theta\theta}/\Delta R$ are similar to those obtained for the ventricle. However, it is worthwhile to note that the effect of increasing the stretch ratio tends to decrease the stiffness at the midwall but increase it at the endocardial surface. This is consistent with the changing stress

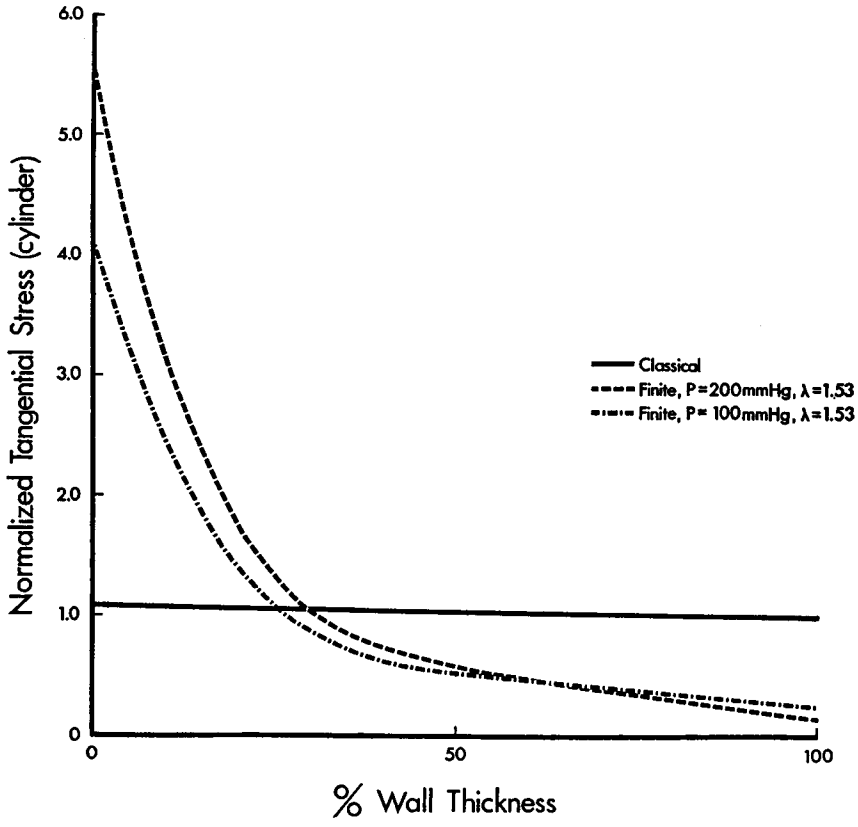

FIGURE 5 Tangential wall stress distributions for a cylindrical artery based on classical and finite theories for a longitudinal stretch ratio $\lambda = 1.53$. Although the arteries are thin walled, the large deformation theory predicts marked stress gradients through the wall in contrast to the uniform distribution as given by the classical theory. The three stress curves shown are normalized to the Laplace stress for a cylinder ($\sigma = PR_1/h$).

patterns observed in Fig. 5 for the stretch ratio $\lambda = 1.53$ at the pressure levels $P = 100$, 200 mm Hg.

Wave Propagation Velocities in Arteries. In previous studies by Mirsky (1968), the wave velocity in arteries was evaluated on the basis of large deformation theory assuming a Mooney material (Green and Zerna, 1954). Such a material is characterized by a strain energy function W which is a linear function of the strain invariants I_1, I_2. In terms of the present notation, the expression for the wave velocity C_{wM} in a Mooney material is given by

$$C_{wM}^2 = (A/\rho)(\Delta P/\Delta A),$$

$$= P(r_2^2 - r_1^2)(R_1^2 r_2^2 + R_2^2 r_1^2)/\lambda^2 \rho R_1^2 R_2^4 D, \qquad (41)$$

where A is the cross-sectional area of the vessel lumen, ρ is the density of the fluid medium (blood) and

$$D = 2 \log_e (R_1 r_2 / R_2 r_1) + (R_2^2 - R_1^2)(R_1^2 - r_1^2/\lambda)/R_1^2 R_2^2.$$

For the present analysis, the wave velocity C_w will be evaluated from the following two expressions:

$$C_{w1}^2 = E_e h / 2\rho R_1 ,$$

$$C_{w2}^2 = (R_1/2\rho)(\Delta P/\Delta R_1), \tag{42}$$

where E_e is the endocardial elastic modulus given by

$$E_e = R_1 \Delta\sigma_{\theta 1}/\Delta R_1 . \tag{43}$$

Since the experimental data for the $P - R_2$ relationship are available from the studies of Simon et al. (1971), the $P - R_1$ data can be readily calculated with the aid of Eqs. 16. These data are given in Table II and the $P - R_1$ relation has been expressed in the exponential form

$$P = 10.2 + 0.0265\, e^{18.4R_1} \quad (\lambda = 1.53), \tag{44}$$

where P is in millimeters of mercury and R_1 in centimeters.

Furthermore $\sigma_{\theta 1}$ is expressed in terms of R_1 by

$$\sigma_{\theta 1} = 59.4 + 0.0663\, e^{21.8R_1} \quad (\lambda = 1.53), \tag{45}$$

where $\sigma_{\theta 1}$ is the endocardial stress based on the classical theory. Note that if P and $\sigma_{\theta 1}$ are expressed in dynes per square centimeter, the wave velocities C_{w1}, C_{w2} are given in centimeters per second.

Fig. 6 shows a plot of the wave velocities C_{wM}, C_{w1}, and C_{w2} as a function of the

TABLE II

PRESSURE-RADIUS DATA FROM THE ARTERIAL STUDIES OF SIMON ET AL.*

P	R_1	R_m	R_2
mm Hg		*cm*	
25	0.348	0.375	0.401
50	0.396	0.420	0.445
75	0.425	0.449	0.473
100	0.442	0.464	0.485
150	0.467	0.489	0.510
200	0.483	0.508	0.524

* The above data are based on a stretch ratio $\lambda = 1.53$.

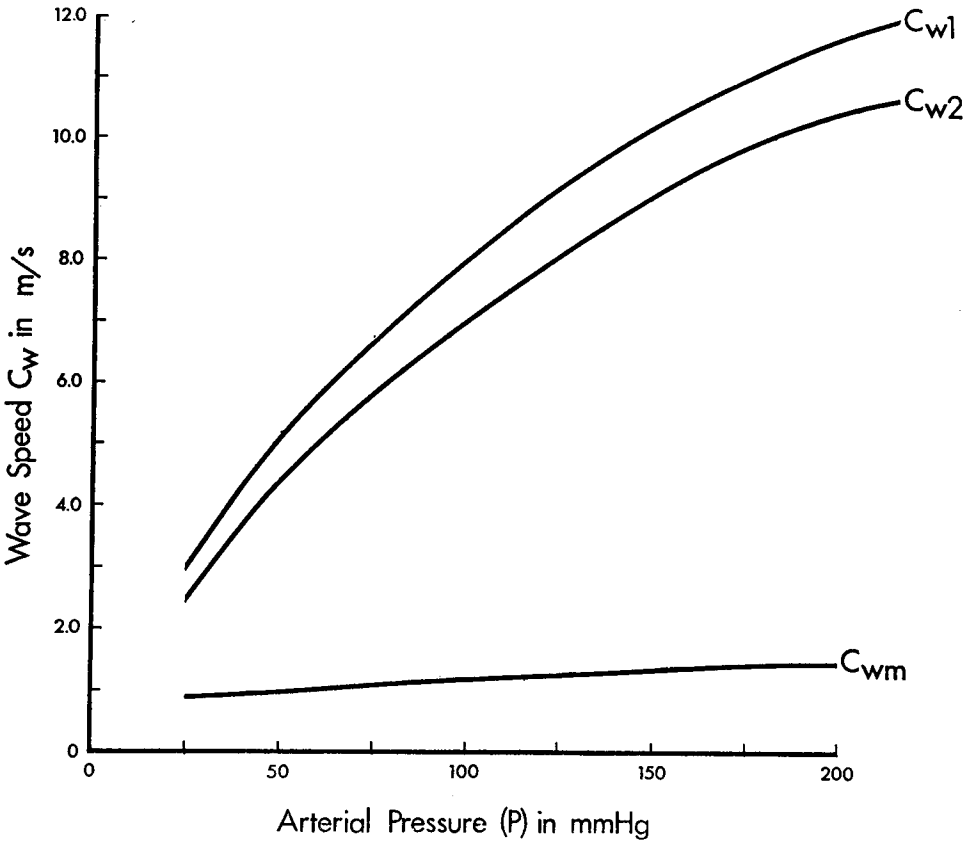

FIGURE 6 The wave propagation velocity C_w is plotted as a function of the arterial pressure. C_{w1} is the wave velocity calculated from the Moens-Korteweg formula $(E_1h/2\rho R_1)^{1/2}$; $C_{w2} = [(R_1/2\rho)\Delta P/\Delta R_1]^{1/2}$ and C_{wM} is the velocity obtained for a Mooney material.

arterial pressure. The wave velocities C_{w1} are approximately 15% higher than C_{w2} and if E_e is replaced by the incremental modulus E_1 (Eq. 40), the resulting wave velocities would be 10% lower than C_{w2}. It is also observed that the velocities C_{wM} for the Mooney material are essentially independent of the pressure and are much lower than those wave velocities observed experimentally (Anliker et al., 1968). In their studies, Simon et al. (1972) obtained the wave velocities by differentiating the integral expression 22 for $L(R_1)$. This analysis appears to be unnecessarily tedious and could be replaced by the previously described procedure, namely (*a*) obtain $L(R_1)$ vs. R_1 relation, and (*b*) curve fit these data to an exponential and then apply the differentiation.

It may be concluded from these analyses that (*a*) marked gradients of stress occur in the endocardial layers of both arteries and ventricles subjected to internal pressures. These high stresses may be responsible for ischemia of the left ventricle and

could be a triggering mechanism for the atherosclerotic lesions (Fry, 1969) frequently observed in human abdominal aortas. Such results are only predicted from a large deformation analysis; (*b*) Laplace's Law even for thin-walled vessels may be open to question since the present theory yields large stress gradients for such structures; (*c*) caution must be exercised in evaluating elastic stiffness from the familiar Moens-Korteweg formula (Eq. 42) for wave velocity since the stiffness varies through the wall and differs for both theories.

Further studies along these lines are necessary in order to better characterize the ventricular response to pressure loading, taking into account fiber orientation and a more appropriate geometry. Finally, methods must be devised to circumvent the problem of obtaining undeformed geometry in both the ventricle and artery if we desire to apply such analyses in the clinical situation.

This work was supported by the grant HL-12711-04 from the National Heart and Lung Institutes of Health.

Received for publication 2 April 1973.

REFERENCES

ANLIKER, M., M. B. HISTAND, and E. OGDEN. 1968. *Circ. Res.* **23**:534.

BARNARD, R. J., R. N. MCALPIN, G. D. BUCKBERG, and A. A. KATTUS. 1972. *Circulation.* **46**(Suppl. 11):73.

BURCH, G. E., C. T. RAY, and J. A. CRONVICK. 1952. *Circulation.* **5**:504.

BURTON, A. C. 1957. *Am. Heart J.* **54**:801.

FRY, D. L. 1969. *Circulation.* **29**(Suppl. IV):38.

FUNG, Y. C. B. 1967. *Am. J. Physiol.* **213**:1532.

GHISTA, D. N., and H. SANDLER. 1969. *J. Biomech.* **2**:35.

GOU, P. F. 1970. *J. Biomech.* **3**:547.

GOULD, P., D. N. GHISTA, L. BROMBOLICH, and I. MIRSKY. 1972. *J. Biomech.* **5**:521.

GREEN, A. E., and J. E. ADKINS. 1960. Large Elastic Deformations. Clarendon Press, Oxford, England.

GREEN, A. E., and W. ZERNA. 1954. Theoretical Elasticity. Clarendon Press, Oxford, England.

LEKHNITSKII, S. G. 1963. Theory of Elasticity of an Anisotropic Elastic Body. Holden-Day, Inc. San Francisco.

MIRSKY, I. 1968. *Bull. Math. Biophys.* **30**:299.

MIRSKY, I. 1969. *Biophys. J.* **9**:189.

MIRSKY, I. 1970. *Bull. Math. Biophys.* **32**:197.

MIRSKY, I., and W. W. PARMLEY. 1972. *Circ. Res.* **33**:233.

MONROE, G., W. J. GAMBLE, C. G. LAFARGE, A. E. KUMAR, J. STARK, G. L. SANDERS, C. PHORNPHUTKUL, and M. DAVIS. 1972. *J. Clin. Invest.* **51**:2573.

PATEL, D. J., and J. S. JANICKI. 1970. *Circ. Res.* **27**:149.

PATEL, D. J., J. S. JANICKI, and T. E. CAREW. 1969. *Circ. Res.* **25**:765.

SANDLER, H., and H. T. DODGE. 1963. *Circ. Res.* **13**:91.

SIMON, B. R., A. S. KOBAYASHI, D. E. STRANDNESS, and C. A. WIEDERHIELM. 1971. *J. Basic Eng.* **93**:138.

SIMON, B. R., A. S. KOBAYASHI, D. E. STRANDNESS, and C. A. WIEDERHIELM. 1972. *Circ. Res.* **30**:491.

SPOTNITZ, H. M., E. H. SONNENBLICK, and D. SPIRO. 1966. *Circ. Res.* **18**:49.

STREETER, D. D., R. N. VAISHNAV, D. J. PATEL, H. M. SPOTNITZ, J. ROSS, JR., and E. H. SONNENBLICK. 1970. *Biophys. J.* **10**:345.

TIMOSHENKO, S., and J. N. GOODIER. 1951. Theory of Elasticity. McGraw-Hill Book Company, New York.

VAISHNAV, R. N., J. T. YOUNG, J. S. JANICKI, and D. J. PATEL. 1972. *Biophys. J.* **12**:1008.
WONG, A. Y. K., and P. M. RAUTAHARJU. 1968. *Am. Heart J.* **75**:649.
WOOD, R. N. 1892. *J. Anat. Physiol. Norm. Pathol. Homme Anim.* **26**:302.

APPENDIX

Development of an Expression for Incremental Modulus in the Sphere and Cylinder

Spherical Case. In the spherical coordinate system (r, θ, φ), the stress-strain relations may be written in the form (Lekhnitskii, 1963)

$$\sigma_{rr} = c_{11}e_{rr} + c_{12}e_{\theta\theta} + c_{12}e_{\varphi\varphi},$$

$$\sigma_{\theta\theta} = c_{12}e_{rr} + c_{11}e_{\theta\theta} + c_{12}e_{\varphi\varphi},$$

$$\sigma_{\varphi\varphi} = c_{12}e_{rr} + c_{12}e_{\theta\theta} + c_{11}e_{\varphi\varphi},$$

where

$$c_{11} = E(1 - \nu)/(1 + \nu)(1 - 2\nu); \qquad c_{12} = E\nu/(1 + \nu)(1 - 2\nu)$$

E being the Young's modulus and ν the Poisson ratio.

Subtraction of the first two equations yields the result

$$\sigma_{\theta\theta} - \sigma_{rr} = (c_{11} - c_{12})(e_{\theta\theta} - e_{rr}) = E(e_{\theta\theta} - e_{rr})/(1 + \nu),$$

$$\text{i.e., } E = (1 + \nu)(\sigma_{\theta\theta} - \sigma_{rr})/(e_{\theta\theta} - e_{rr}).$$

For an incompressible material, $\nu = 0.5$ hence the incremental modulus is given by

$$E_{\text{INC}} = (3/2)(\Delta\sigma_{\theta\theta} - \Delta\sigma_{rr})/(\Delta e_{\theta\theta} - \Delta e_{rr}).$$

Furthermore, the incompressibility condition requires that $e_{rr} + e_{\theta\theta} + e_{\varphi\varphi} = 0$, hence $\Delta e_{rr} = -\Delta e_{\theta\theta} - \Delta e_{\varphi\varphi} = -2\Delta e_{\theta\theta}$ and the above expression reduces to

$$E_{\text{INC}} = (\Delta\sigma_{\theta\theta} - \Delta\sigma_{rr})/2\Delta e_{\theta\theta}.$$

Cylindrical Case. For the cylindrical coordinate system (r, θ, z) the stress-strain relations are given by

$$\sigma_{rr} = c_{11}e_{rr} + c_{12}e_{\theta\theta} + c_{12}e_{zz},$$

$$\sigma_{\theta\theta} = c_{12}e_{rr} + c_{11}e_{\theta\theta} + c_{12}e_{zz},$$

$$\sigma_{zz} = c_{12}e_{rr} + c_{12}e_{\theta\theta} + c_{11}e_{zz}.$$

On subtracting the first two relations we obtain

$$(\sigma_{\theta\theta} - \sigma_{rr}) = E(e_{\theta\theta} - e_{rr})/(1 + \nu)$$

and the incremental modulus for an incompressible material is again given in the form

$$E_{\text{INC}} = (3/2)(\Delta\sigma_{\theta\theta} - \Delta\sigma_{rr})/(\Delta e_{\theta\theta} - \Delta e_{rr}).$$

For the cylindrical case, the incompressibility condition requires that $e_{rr} + e_{\theta\theta} + e_{zz} = 0$ i.e., $\Delta e_{rr} + \Delta e_{\theta\theta} + \Delta e_{zz} = 0$. However, it was assumed that the cylinder length remains constant after the initial stretch. Thus e_{zz} = constant, $\Delta e_{zz} = 0$, $\Delta e_{rr} = -\Delta e_{\theta\theta}$ and the incremental modulus expression reduces to

$$E_{\text{INC}} = (3/4)(\Delta\sigma_{\theta\theta} - \Delta\sigma_{rr})/\Delta e_{\theta\theta}\,.$$